# Shape Design Optimization for Viscous Flows in a Channel with a Bump and an Obstacle

Henry Kasumba
Institute of Mathematics and
Scientific Computing
Karl-Franzens University, Graz
Graz, Austria A-8010
Email: henry.kasumba@uni-graz.at

Karl Kunisch
Institute of Mathematics and
Scientific Computing
Karl-Franzens University, Graz
Graz, Austria A-8010
Email: karl.kunisch@uni-graz.at

***Abstract*— A shape design optimization problem for viscous flows in an open channel with a bump and an obstacle are investigated. An analytical expression for the shape design sensitivity involving different cost functionals is derived using the adjoint method and the material derivative concept. A channel flow problem with a bump as a moving boundary is taken as an example. The shape of the bump, represented by Bezier curves of order 3, is optimized in order to minimize the vortices in the flow field. Numerical discretizations of the primal (flow) and adjoint problems are achieved using the Galerkin FEM method. Numerical results are provided in various graphical forms at relatively low Reynolds numbers. Striking differences are found for the optimal shape control corresponding to the 3 different cost functionals, which constitute different quantifications of vorticity.**

## I. Introduction

An important topic in the field of optimal control of partial differential equation is the choice of appropriate cost function which is used to quantify the control objective. This functional depends on the state variables $(u, p)$, where $u$ and $p$ are the velocity and pressure of the fluid respectively and in our case on the control parameters describing the shape of the domain. Typical cost functionals that are in use today for vortex reduction, are based on tracking-type functionals or minimization of the curl of the velocity field. i.e.

$$J_1(u) = \int_{\tilde{\Omega}} |u(x) - u_d(x)|^2 \, dx, \quad J_2(u) = \int_{\tilde{\Omega}} |\text{curl } u(x)|^2 \, dx, \tag{1}$$

where $\tilde{\Omega} \subset \Omega$ describes the subset of $\Omega$ over which vortex reduction is desired and $u_d$ stands for a given desired flow field which contains some of the expected features of the controlled flow field without the undesired vortices. These functionals, have the disadvantage that they are not invariant under changes of frames which move at a constant speed relative to each other. Functionals which allow such a property are referred to as **Galilean invariant**. A functional based on Galilean invariant vortex definition is given by

$$J_3(u) = \int_{\tilde{\Omega}} \max(0, \det \nabla u(x)) \, dx. \tag{2}$$

Due to the max-operation the cost functional in (2) is not differentiable and hence we introduce the smoothing function $g_3 \in C^2(\mathbb{R})$ defined e.g. by $g_3(t) = \begin{cases} 0, & t \leq 0 \\ t^3/(t^2+1), & t > 0 \end{cases}$, such that

$$J_3(u) = \int_{\tilde{\Omega}} g_3(\det \nabla u(x)) \, dx. \tag{3}$$

A first step towards investigating Galilean invariant cost-functional for optimal control in fluids was carried out in [1] for a flow around an obstacle. In this case striking differences were found for the optimal controls corresponding to the three different cost functionals expressed in (1-2). In this work the authors systematically analyze optimal shapes corresponding to the minimization of functionals (1-2). A comparison among the three cost functionals is made using two test problems. The first test problem consists in minimization of vorticity in flows in an open channel with a bump and the second test example consists in minimization of vorticity in an open channel with an obstacle. In order to use gradient type methods, the characterization of the shape gradients for all three functionals is achieved. The continuous formulations are discretized and numerical algorithms for solving the discrete shape optimization problem are developed and implemented.

## II. Setting of the problem

### A. State problem

Let $\Omega \subset \mathbb{R}^2$ with a sufficiently regular boundary $\Gamma$. Suppose that an incompressible viscous flow occupies $\Omega$, and that the state equation for the flow is given by the following system of Navier-Stokes equations in non-dimensional form:

$$\begin{cases} -\frac{1}{Re}\Delta u + u \cdot \nabla u + \nabla p = f \ \text{ in } \ \Omega, \\ \text{div } u = 0 \ \text{ in } \ \Omega, \end{cases} \tag{4}$$

where $u, p$ and $Re$ are the velocity, pressure and Reynold's number of the flow. We consider two typical problems described in Figure 1 where in both problems, the boundary $\Gamma_f$ is used as a control boundary by means of which the shape of $\Omega$ will be governed. The boundary conditions for the test problems are given as follows

$$\begin{cases} u = g \ \text{ on } \ \Gamma_{in}, \\ u = 0 \ \text{ on } \ \Gamma_w \cup \Gamma_f, \\ -pn + \frac{1}{Re}\frac{\partial u}{\partial n} = 0 \ \text{ on } \ \Gamma_{out}. \end{cases} \tag{5}$$

978-1-4244-7827-9/10/$26.00 ©2010 IEEE

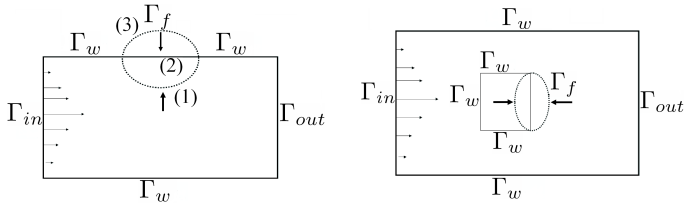


*(a) Problem 1* *(b) Problem 2*

Fig. 1. Domains for test problems

### *B. Optimization problem*

Our goal is to find "an optimal" $\Gamma_f$ by minimizing the cost functionals (1-2) which depend on $(\Omega, u, p)$ which is a solution to (4-5). The optimization problem can be written in the following form:

$$\begin{cases} \text{Find } \Gamma_f^* \in \mathcal{U}_{ad} \text{ such that} \\ J(\Omega(\Gamma_f^*), u(\Gamma_f^*)) \leq J(\Omega(\Gamma_f), u(\Gamma_f)) \quad \text{for all} \quad \Gamma_f \in \mathcal{U}_{ad}. \end{cases} \tag{6}$$

To describe $\mathcal{U}_{ad}$, we let $\Gamma_f$ be described as a graph represented by the curve $\alpha : [a, b] \mapsto \mathbb{R}$ which we assume is given by

$$\Gamma_f(\alpha) = \{(x_1, x_2) : \ x_1 \in [a, b], \ x_2 = [c, \alpha(x_1)]\}. \tag{7}$$

for problem 1 and

$$\Gamma_f(\alpha) = \{(x_1, x_2) : , x_1 = [f, \alpha(x_2), \ x_2 \in [d, e]]\}, \tag{8}$$

for problem 2 where $a, b, c, d, e, f$ are given constants. Consequently one may define the admissible family of curves defining $\Gamma_f(\alpha)$ for problem 1 as follows:

$$\mathcal{U}_{ad} = \{\alpha \in C^{1,1}([a, b]) \ \Big| \ 0 < \alpha_{min} \leq \alpha(x_1) \leq \alpha_{max}, \\ \alpha(a) = \alpha_0, \alpha(b) = \alpha_1, |\alpha'| \leq L_1, \text{ a.e in } (a, b)\}.$$

Similarly we can define $\mathcal{U}_{ad}$ for problem 2. We define the convergence in $\mathcal{U}_{ad}$ as follows

$$\alpha_n \rightsquigarrow \alpha \triangleq \alpha_n \rightrightarrows \alpha \text{ in } [a, b]. \tag{9}$$

From the well known Arzelà-Ascoli theorem it follows that $\mathcal{U}_{ad}$ is compact with respect to the above defined convergence. Hence to establish existence of solution to (6) one needs to use the classical Bolzano-Weierstrass theorem for continuous functions on compact sets.(see e.g. [2] for details)

## III. Sensitivity analysis

In this section we discuss the necessary optimality conditions for (6). The derivation is rigorous for $J_1, J_2$, but only formal for $J_3$. In order to set up the optimality system, a common technique is to introduce a family of perturbations $\Omega_t$ of a given admissible domain $\Omega$ which depend on a parameter $t$. It can be constructed for instance by perturbation of the identity. Let $\Omega \subset \bar{D}$ be open and let

$$\mathcal{H} = \{\mathbf{h} \in C^{1,1}(\bar{D}) : \mathbf{h}|_{\partial D} = 0\} \tag{10}$$

be the space of deformation fields which define for $t > 0$ a perturbation of $\Omega$ by

$$T_t : D \mapsto \mathbb{R}^d, \tag{11}$$

$$x \mapsto T_t(x) = x + t\mathbf{h}(x). \tag{12}$$

Then for each $\mathbf{h} \in \mathcal{H}$, there exists $\tau > 0$ such that $T_t(D) = D$ and $\{T_t\}$ is a family of $C^{1,1}$-diffeomorphisms for $|t| < \tau$. For each $t \in \mathbb{R}$ with $|t| < \tau$, we set

$$\Omega_t = T_t(\Omega), \quad \Gamma_t = T_t(\Gamma).$$

Thus $\Omega_0 = \Omega, \Gamma_0 = \Gamma, \Omega_t \subset D$. The Eulerian derivative of $J$ at $\Omega$ in the direction of the deformation field $\mathbf{h}$ is defined as

$$dJ(u, \Omega)\mathbf{h} = \lim_{t \to 0} \frac{J(u_t, \Omega_t) - J(u, \Omega)}{t}. \tag{13}$$

To derive (13), we shall consider the following general optimization problem

$$\min_{\Omega \in \mathcal{U}_{ad}} J(u, \Omega) \equiv \int_\Omega J_1(C_\gamma u) dx, \tag{14}$$

subject to the constraint

$$E(u, \Omega) = 0, \quad u \in X \tag{15}$$

$X \subset L^2(\Omega)^l$, $l \in \mathbb{N}$, a Hilbert space with a dual $X^*$, $E(u, \Omega) = 0$ represents a partial differential equation posed on a domain $\Omega$ and $C_\gamma$ is an affine operator:

$$C_\gamma : u(\cdot) \mapsto Cu(\cdot) + \gamma(\cdot) \qquad \gamma \in L^2(\Omega)$$

and $C \in \mathcal{L}(X, L^2(\Omega))$ is a linear differential operator.

Any function $u_t : \Omega_t \mapsto \mathbb{R}^l$, for some $l \in \mathbb{N}$, can be mapped back to the reference domain by

$$u^t = u_t \circ T_t : \Omega \mapsto \mathbb{R}^l. \tag{16}$$

From the chain rule it follows that the gradients of $u_t$ and $u^t$ are related by

$$\nabla u_t \circ T_t = (DT_t)^{-T} \nabla u^t, \tag{17}$$

and $u^t : \Omega \mapsto \mathbb{R}^l$ satisfies the equation on the reference domain which we express as

$$\tilde{E}(u^t, t) = 0, \quad |t| < \tau. \tag{18}$$

Because $T_0 = id$, one obtains $u^0 = u$ and

$$\tilde{E}(u^0, 0) = E(u, \Omega). \tag{19}$$

The following lemma is needed

*Lemma 3.1:* There is a constant $c > 0$, such that

$$|J_1(C_\gamma v) - J_1(C_\gamma u) - \big(J_1'(C_\gamma u)(v-u), C(v-u)\big)|_{L^1} \leq c|C(v-u)|_{L^2}^2 \tag{20}$$

hold for all $v, u \in X$.

The adjoint state $p \in X$ is defined as the solution to

$$\langle E_u(u, \Omega)\psi, p\rangle_{X^* \times X} = (C^* J_1'(C_\gamma u), \psi) \quad \text{for all } \psi \in X \tag{21}$$

In IKP [3], the following assumptions (H1-H4) were imposed on $\tilde{E}$, respectively $E$:

(H1) There is a $C^1$-function $\tilde{E} : X \times (-\tau, \tau) \mapsto X^*$ such that $E(u_t, \Omega_t) = 0$ is equivalent to

$$\tilde{E}(u^t, t) = 0 \ \text{ in } X^*,$$

with $\tilde{E}(u, 0) = E(u, \Omega)$ for all $u \in X$.

(H2) There exists $0 < \tau_0 \leq \tau$ such that for $|t| < \tau_0$, there exists a unique solution $u^t \in X$ to $\tilde{E}(u^t, t) = 0$ and

$$\lim_{t\to 0} \frac{|u^t - u^0|_X}{|t|^{\frac{1}{2}}} = 0.$$

(H3) $E_u(u, \Omega) \in \mathcal{L}(X, X^*)$ satisfies

$$\langle E(v, \Omega) - E(u, \Omega) - E_u(u, \Omega)(v - u), \psi\rangle_{X^*\times X} = \mathcal{O}(|v - u|_X^2).$$

(H4) $\tilde{E}$ and $E$ satisfy

$$\lim_{t\to 0} \frac{1}{t}\langle \tilde{E}(u^t, t) - \tilde{E}(u, t) - E(u^t, \Omega) + E(u, \Omega), \psi\rangle_{X^*\times X} = 0.$$

With regards to the cost functional $J$, we require:

(H5) $J_1 \in C^{1,1}(\mathbb{R}^l, \mathbb{R})$

Condition (H5) implies that $J_1(C_\gamma u) \in L^2(\Omega, \mathbb{R})$ and $J_1'(C_\gamma u) \in L^2(\Omega, \mathbb{R}^l)$ for $u \in L^2(\Omega, \mathbb{R}^l)$. Hence $J(u, \Omega)$ is well defined for every $u \in X$. We shall utilize the following additional assumption:

(H6)
$$\begin{cases} \text{There exists a matrix } A_t \text{ such that} \\ t \mapsto A_t \in C(\tau, C(\bar{D}, \mathbb{R}^{d\times d})) \text{ and} \\ C_\gamma u_t \circ T_t = A_t C u^t + \gamma, \\ C_\gamma(u \circ T_t^{-1}) = A_t C u \circ T_t^{-1} + \gamma, \\ \lim_{t\to 0} \frac{A_t - I}{t} \text{ exists, } A_t|_{t=0} = I. \end{cases}$$

*Theorem 3.1:* If (20) and (H1-H6) hold and $J_1(u) = |u|^2$, then the Eulerian derivative of $J$ in the direction $\mathbf{h} \in C^{1,1}(\bar{D}, \mathbb{R}^d)$ exists and is given by the expression

$$dJ(u, \Omega)\mathbf{h} = -\frac{d}{dt}\langle \tilde{E}(u, t), p\rangle_{X^*\times X}|_{t=0} + \int_\Gamma J_1(C_\gamma u)\mathbf{h}\cdot n \, ds - \left(J_1'(C_\gamma u), C\nabla u^T \cdot \mathbf{h})\right)_\Omega.$$

We can show that all conditions (H1-H6) are satisfied by system (4-5) and hence using Theorem 3.1, we can show that the Eurelian derivative of the cost functions in (1) can be expressed in the form

$$dJ(u, \Omega)\mathbf{h} = \int_{\Gamma_f} \nabla J_i \mathbf{h}\cdot n \, ds, \quad i = 1, 2,$$

where

$$\nabla J_1 = \left[\frac{1}{2}|u - u_d|^2 + \frac{1}{Re}(Du\cdot n)\cdot(D\lambda\cdot n)\right],$$

$$\nabla J_2 = \left[\frac{1}{2}|\text{curl } u|^2 + (Du\cdot n)\cdot\left(\frac{1}{Re}D\lambda\cdot n - \text{curl } u\cdot\tau\right)\right],$$

and $\lambda$ is a solution to the following adjoint equation

$$\begin{cases} -\frac{1}{Re}\Delta\lambda - D\lambda\cdot u + (Du)^t\cdot\lambda + \nabla q = J_i(u)' \ \text{ in } \ \Omega, \\ \text{div } \lambda = 0 \ \text{ in } \ \Omega, \\ \lambda = 0 \ \text{ on } \ \Gamma_w \cup \Gamma_f \cup \Gamma_{in}, \\ q\cdot n - \alpha\nabla\lambda\cdot n - (u\cdot n)\lambda = 0 \ \text{ on } \ \Gamma_{out}. \end{cases}$$

Using formal arguments, we can also show that for a smooth boundary, the representation (III) holds for $J_3$ and

$$\nabla J_3 = \left[g_3(\det\nabla u) + (Du\cdot n)\cdot\left(\frac{1}{Re}(D\lambda\cdot n) - P(u)\right)\right],$$

where

$$P(u) = \begin{pmatrix} g_3'(\det\nabla u)\left(\frac{\partial u_2}{\partial x_2}\cdot n_x - \frac{\partial u_2}{\partial x_1}\cdot n_y\right) \\ g_3'(\det\nabla u)\left(\frac{\partial u_1}{\partial x_1}\cdot n_y - \frac{\partial u_1}{\partial x_2}\cdot n_x\right) \end{pmatrix}.$$

## IV. Finite element approximation and discretization

The following functional spaces are chosen

$$H_g^1 = \{[H^1(\Omega)]^2 | u = g \text{ on } \Gamma_{in}, u = 0 \text{ on } \Gamma_w \cup \Gamma_f\},$$
$$H_0^1 = \{v \in [H^1(\Omega)]^2 |, u = 0 \text{ on } \Gamma_{in} \cup \Gamma_w \cup \Gamma_f\}.$$

Then weak formulation of the state system reads as follows: Find $(u, p) \in H_g^1(\Omega) \times L^2(\Omega)$ such that for all $(\psi, \xi) \in H_0^1(\Omega) \times L^2(\Omega)$ :

$$\begin{cases} \int_\Omega \left(\frac{1}{Re}\nabla u\nabla\psi + (u\cdot\nabla)u\psi - p \ div \ \psi\right) dx = \int_\Omega f\psi \ dx, \\ \int_\Omega \text{div } u \ \xi \ dx = 0, \end{cases}$$

and that of the adjoint system reads:
Find $(\lambda, q) \in H_0^1(\Omega) \times L^2(\Omega)$ such that for all $(\psi, \xi) \in H_0^1(\Omega) \times L^2(\Omega)$:

$$\begin{cases} \int_\Omega \left(\frac{1}{Re}\nabla\lambda\nabla\psi + (\psi\cdot\nabla)u\lambda + (u\cdot\nabla)\psi\lambda - div\psi \ q\right)dx = \int_\Omega \frac{\partial J_i}{\partial u} \ \psi \ dx, \\ \int_\Omega \text{div } \lambda \ \xi \ dx = 0. \end{cases}$$

We project the spaces $H_g^1(\Omega), H_0^1(\Omega)$ and $L^2(\Omega)$ into finite dimensional subspaces $V_{gh}, V_{0h}$ and $S_h$. This is accomplished by spatial discretization of the domain $\Omega$ to obtain the following two families of finite dimensional subspaces

$$V_{gh} := \{u_h \in X_h : u_h = 0 \ on \ \Gamma_w \cup \Gamma_f, \ u_h = g \ on \ \Gamma_{in}\},$$
$$V_{0h} := \{u_h \in X_h : u_h = 0 \ on \ \Gamma_w \cup \Gamma_f \cup \Gamma_{in}\},$$

where $X_h \subset H^1(\Omega)^2$ and $S_h \subset L^2(\Omega)$.
The Galerkin approximation of the state system then reads as follows:
Find $(u_h, p_h) \in V_{gh} \times S_h$ such that for all $(\psi_h, \xi_h) \in V_{0h} \times S_h$

$$\begin{cases} \int_{\Omega_h} \left(\frac{1}{Re}\nabla u_h\nabla\psi_h \ + (u_h\cdot\nabla)u_h\psi_h - p_h div \ \psi_h\right) dx = \int_{\Omega_h} f\psi_h \ dx, \\ \int_{\Omega_h} \text{div } u_h \ \xi_h \ dx = 0, \end{cases}$$

and that of the adjoint state system reads:
Find $(\lambda_h, q_h) \in V_{0h} \times S_h$ such that for all $(\psi_h, \xi_h) \in V_{0h} \times S_h$

$$\begin{cases} \int_{\Omega_h} \left(\frac{1}{Re}\nabla\lambda_h\nabla\psi_h + (\psi_h\cdot\nabla)u_h\lambda_h \right. \\ \left. +(u_h\cdot\nabla)\psi_h\lambda_h - \text{div } \psi_h q_h\right) dx = \int_{\Omega_h} \frac{\partial J_{i,h}}{\partial u} \ \psi_h \ dx, \\ \int_{\Omega_h} \text{div } \lambda_h\xi \ dx = 0. \end{cases}$$

By choosing appropriate basis for the velocity and pressure space, in particular polynomials of degree 2 for the velocity

space and polynomials of degree 1 for the pressure space. The resulting algebraic equations can finally be solved. The non-linearity in the Navier-Stokes equations is linearized using the Picard method. At each step of the Picard loop, the linearized discrete problem is solved using a multi-frontal Gauss LU factorization implemented in the package `UMFPACK`. [1]

## V. Iterative methods using the discrete shape gradient

We have seen that

$$dJ(u,\Omega)\mathbf{h} = \int_{\Gamma_f} \nabla J\mathbf{h}\cdot n\ ds. \tag{22}$$

This suggests to use $\mathbf{h} = -\nabla J n$ as gradient descent direction and to move the boundary in direction $\mathbf{h}$. However it is not clear if optimal shapes, if they exist, are smooth enough. Moreover the normal $n$ is always less smooth than the parametrization. Therefore we need to smooth the decent direction. We can do so by using the so called Sobolev gradient instead of the $L^2$ gradient and this amount to changing the scalar product with which we compute the velocity field e.g $H^1(\Omega)$. This procedure moreover has an effect of preconditioning of the descent direction as well as extending $\mathbf{h}$ over the whole domain.

### A. The boundary variation algorithm

1. Choose initial shape $\Omega_0$;
2. Compute the state system and the adjoint system , then evaluate the descent direction $\mathbf{h}_k$ by using

$$-\Delta\mathbf{h} + \mathbf{h} = 0 \ \text{ in } \ \Omega, \tag{23}$$

$$\frac{\partial \mathbf{h}}{\partial n} = -\nabla J\ n \ \text{ on } \Gamma_f, \tag{24}$$

$$\mathbf{h} = 0 \ \text{ on } \Gamma_{in}\cup\Gamma_w\cup\Gamma_{out}, \tag{25}$$

   with $\Omega = \Omega_k$;
3. Set $\Omega_{k+1} = (Id + t_k\mathbf{h}_k)\Omega_k$ where $t_k$ is a small positive scalar, chosen using some step size rule .

Then $dJ(\Omega,\mathbf{h}) = \int_{\Gamma_f} \nabla J\mathbf{h}\cdot n\ ds = -\int_{\Omega} |\nabla\mathbf{h}|^2 + |\mathbf{h}|^2 dx < 0$

which again guarantees a descent direction.

## VI. Numerical examples

We now give selected numerical results.

### A. Flow in a channel with a bump

In this example, the study of the optimization of a flow in a channel with a bump as shown in Fig. 1(a) is presented. The dimensions of the channel are as follows, $-1 < x < 1$ and $-1 < y < 1$ with a bump on the upper wall extending from $x = -0.5$ to $x = 0.5$, i.e. $a = -0.5, b = 0.5$ in $\mathcal{U}_{ad}$ and $g = 2.5(y+1)(1-y), 0)$. The bump which is the free boundary in this case is determined as a sum of Bezier polynomials of degree three so that the bump continuously meets the straight channel wall on either side of it. The computational domain is discretized by triangular elements generated by a bi-dimensional anisotropic mesh generator. $Re$ is set to 50 and the Navier-Stokes equations are solved using a Picard type iteration. The following figure (2) for the velocity field is obtained. The flow field pattern (figure (2)) posses a vortex in

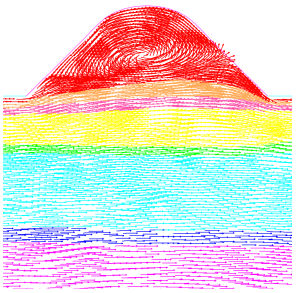

*zoomed*

Fig. 2. Vector plot of velocity vectors $u_1$ and $u_2$

the hump of the computational domain. This is what we want to reduce/minimize by using the freely moving boundary part of the domain ($\Gamma_f$) as the control.

*1) Choice of boundary conditions:* The choice of boundary condition for this example ensures that the solution of (4-5) has a parabolic profile if $\Omega$ is a square. More precisely, if $\Omega$ is a square $[-1,1]\times[-1,1]$, the solution is given by:

$$\begin{cases} u(x,y) = (2.5(y+1)(1-y), 0), \\ p(x,y) = \frac{5}{Re}(1-x). \end{cases} \tag{26}$$

### B. Shape optimization with cost $J_1$

The desired state is chosen as $u_d = (2.5(y+1)(1-y), 0)$. With this choice of target flow, the functional $J_1$ vanishes at the optimal domain, which in this case is known to be a square. We start the algorithm with initial flow as in figure (2). We set some particular number of iterations, in this case 15 as the stopping criterion. If it is too small, we restart the algorithm, with the previous shape as the initial shape until our algorithm stagnates, then we stop. Stagnation is determined by a combination of the values of $dJ(\Omega)\mathbf{h}$ and visual inspection.

*1) Results:* In Figure (3) we display the results that we obtain after optimization The value of the cost $J_1$ on the

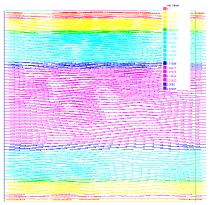

Fig. 3. velocity field on final geometry

initial geometry is $0.118577$ while that on the final geometry is found to be $1.97727e^{-11}$. As expected, the flow field on the optimal geometry has a parabolic flow profile with no vortices as shown in figure(3). A plot of the history of the three cost functions during the minimization process according to $J_1$ results in figures (4 a-c). From these figures, we see

[1] http:// www.netlib.org/linalg

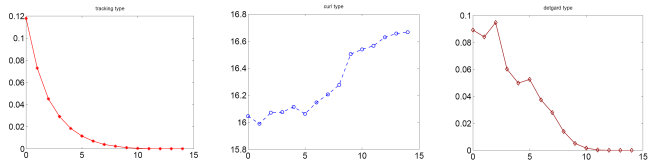

*a)History of $J_1$* *b)History of $J_2$* *c)History of $J_3$*

Fig. 4. velocity on final geometry

that as the number of iterations increases, both cost $J_1$ and $J_3$ decrease while $J_2$ increases. This means that the optimal geometry which minimizes both $J_1$ and $J_3$ is not the optimal one for $J_2$.

### C. Shape optimization with cost $J_2$

The results from the previous subsection indicate that the optimal geometry which minimizes $J_2$ is not a square. In this

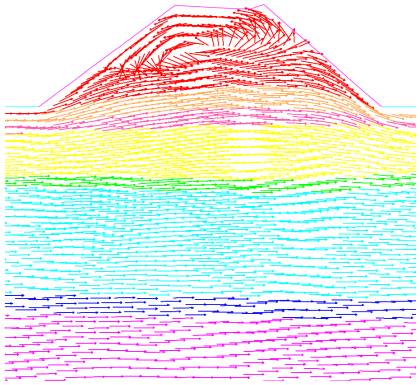

Fig. 5. zoomed final flow

case initialization is made with geometry $\Omega_0$ with a bump in position (1) (see Figure (1 (a))) and the value of the cost on $\Omega_0$ is 32.69. After 14 iterations, the value of the cost on the final design is 16.0 which gives a relative reduction of $50.87\%$ of the initial cost. From figure (5), we see that although we have reduced the value of the cost functional $J_2$ in a mathematical point of view, we have created a vortex. From a physical point of view, energy is applied to overcome the effect of the wall where no slip boundary condition holds. That energy loss is proportional to the normal gradient of the tangential velocity component at the wall. Compared to our example, this gradient is reduced by separation giving results shown in Figure (5 ). Hence this shows that in this particular example, cost functional $J_2$ seems not to be a good candidate for vortex reduction in this shape optimization problem.

### D. Shape optimization with cost $J_3$

Similar results as in the case of $J_1$ are obtained by $J_3$(see figure 3)

*We remark here that the optimal geometry obtained when using the tracking type cost functional depends on how we define the desired flow $u_d$. A different choice other than the parabolic flow profile will yield a different optimal geometry.*

We come to the conclusion that the cost functional $J_3$ seems a better choice at least in this particular example of minimize the vortex in the channel flow with a bump on one of the boundaries.

## VII. Flow in a channel with an obstacle

In this subsection, we want to reduce the vortex shedding behind an obstacle placed in a parallel channel by changing the shape of one of its boundaries. The cost criteria are again the three cost functionals introduced in the previous sections. In this example, the exact solution to this flow problem is not known, which means that the optimal shape which minimizes either of the three cost functionals is not known apriori. Due to the fact that the cost functionals are non-convex, the initialization of the algorithm can be important. We perform a direct numerical simulation for different geometries and we compute the value of each of the three cost functionals on these geometries. The geometry which gives the least cost will be used as the initial guess for the boundary variation algorithm.

### A. Computational geometries and direct numerical simulation

Three of the possible initialization configurations for $\Gamma_f$ (refer to Fig.1. problem 2 ) are considered. The resulting computational domains are then discretized by triangular elements generated by a bi-dimensional anisotropic mesh generator. The boundary conditions are set as in (5) where $g = (1.2(0.5-y)(y+0.5), 0)$. The Reynold's number $Re$ is set equal to 120. All computations are performed using FreeFem++ a variational penalty-based solver, penalty 1e30. The following flow field patterns in Figure (6) are obtained. After computation of the numerical solution in each of the

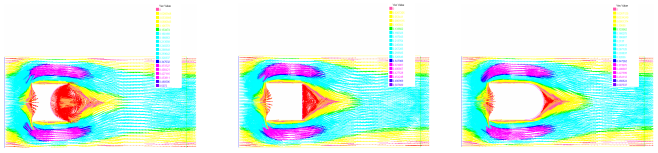

(a) Geom 1 (b) Geom 2 (c) Geom 3

Fig. 6. Vector plots of flow field patterns

three cases we evaluate the values of each of the three cost functionals. In table (I), we report the results obtained . In each

| Geom | Cost $J_1$ (Tracking) | Cost $J_2$ (Curl) | Detgrad cost $J_3$ |
|---|---|---|---|
| 1 | 0.0567474 | 3.96193 | 0.329811 |
| 2 | **0.0565549** | **3.95435** | 0.327914 |
| 3 | 0.0577802 | 4.25205 | **0.310867** |

TABLE I

The values of the cost functions on the three geometries

column, we mark with bold font the least value of the cost obtained after evaluation on each of the three geometries, e.g, for the tracking type cost, the second geometry gives the least value of this cost functional and so on. Now that we have some idea of where the optimal geometry of each of the three cost functional lie, the task now is to use a numerical optimization

procedure to find the optimal shapes that minimize each of the three cost functionals.

### B. Optimization with Tracking cost $J_1$

The desired state is chosen as $u_d = (0.07(0.5-y)(y+0.5), 0)$. This choice of the desired state is motivated by the fact that we want to supress the vortex in the flow around the obstacle. We start the optimization from the geometry that gives a minimum cost after direct numerical simulation. (c.f. Table I). In this case we start with discretized geometry with an initial flow as in (figure 6 b) and we use the boundary variation algorithm already explained in the previous section. The following results are obtained. In figure (7) we show the flow field on

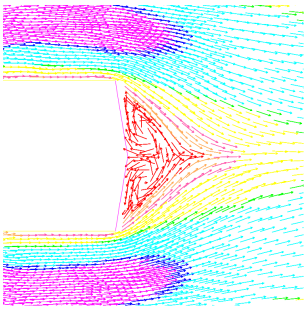

Fig. 7. Zoomed velocity field on optimal geometry

the final geometry obtained after 17 iterations. The value of the cost on the initial geometry is found to be 0.0577918 while that on the final geometry is found to be 0.0564491. Although the cost has been reduced relatively by $2.3\%$, the flow field on the final geometry still possess a vortex. We remark that the optimization using this cost depends upon the definition of the desired state, i.e. different desired state values $u_d$ yield different optimal shapes.

### C. Optimization with curl type cost $J_2$

In this subsection, we find an optimal shape that minimizes the curl type cost functional subject to the Navier-Stokes system. We start the optimization from the geometry that give a minimum cost after direct numerical simulation. (c.f. Table I). In this case we start with discretized geometry with an initial flow as in (figure (6) b). The following results are obtained,

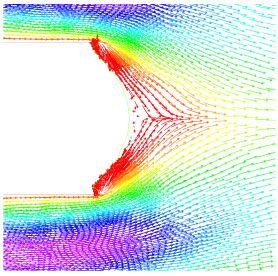

Fig. 8. Zoomed velocity field on optimal geometry

In figure ((8)) we show the flow field on the final geometry. The value of the cost on the initial geometry is 3.95709 while that on the final geometry is found to be 3.91294. The gives a relative reduction of $1.1137\%$ in the value of the cost. However still small vortices are still visible on a micro scale in this case near the corners where $\Gamma_f$ means the fixed boundaries $\Gamma_w$ of the embedded obstacle.

### D. Optimization with cost $J_3$

In this subsection, we minimize cost functional $J_3$, subject to the Navier-Stokes system. We start the computation with the initial geometry $\Omega_0$ with a flow as shown in figure (6(c)). The value of the cost $J_3$ on $\Omega_0$ is found to be $0.311156$ (c.f

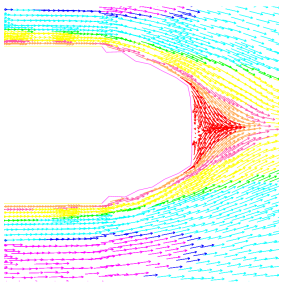

Fig. 9. Zoomed velocity field on optimal geometry

table I) while that on $\Omega_{\text{opt}}$ (figure 9) is found to be 0.2994 and this gives a relative reduction of $3.7782\%$ in the value of the cost after 17 iterations. Results from minimization of $J_3$ further indicate a visual reduction in the vortex from the practical point of view.

## VIII. Conclusions

Our results confirm that the choice of cost functional is important for vortex reduction in fluid dynamics. Galilean invariant cost functionals should be preferred over functionals which are not galilean invariant.


## Acknowledgment

The authors would like to thank Prof. Brenn from the Technical University of Graz for a very helpful discussion.


## References


[1] K. Kunisch and B. Vexler, "Optimal vortex reduction for instationary flows based on translation invariant cost functionals," *SIAM J. Control Optim*, vol. 46, no. 4, pp. 1368–1397, Sept. 2007.

[2] M. D. Gunzburger and H. Kim, "Existence of an optimal solution of a shape control problem for the stationary navier–stokes equations," *SIAM J. Control Optim*, vol. 36, pp. 895–909, May 1998.

[3] K. Ito, K. Kunisch, and G. H. Peichl, "Variational approach to shape derivatives," *ESAIM: COCV*, vol. 14, no. 3, pp. 517–539, 2008.